Experimental Rate Measurements for NS + NO, O_2 and NO_2, and Electronic Structure Calculations of the Reaction Paths for NS + NO_2†

Mark A. Blitz, Kenneth W. McKee, and Michael J. Pilling*

School of Chemistry, University of Leeds, Leeds LS2 9JT, U.K.

Mark A. Vincent and Ian H. Hillier

Chemistry Department, University of Manchester, Manchester M13 9PL, U.K.

Received: January 10, 2002; In Final Form: June 28, 2002

This study reports the first direct kinetic measurements on the NS radical. NS was produced by photolysis of N_4S_4 at 248 nm and was detected via laser-induced fluorescence. A fast reaction was observed between NS and NO_2, with $k = (2.54 \pm 0.12) \times 10^{-11}$ cm^3 molecules^{-1} s^{-1} (error = 2σ including systematic errors) at 295 K. The rate coefficient shows a small negative temperature dependence over the range 295−673 K, which is represented by $k = (2.57 \pm 0.11) \times 10^{-11}(T/295\ \mathrm{K})^{-1.10\pm0.10}$ cm^3 molecule^{-1} s^{-1}. The reaction was also investigated using density functional theory (B3LYP/6-31G**) to calculate the geometries of the stationary points on the potential energy surface, coupled with Brueckner doubles and perturbative triples to determine energy differences. The calculations show a direct route from reactants to N_2 + SO_2, via a series of isomers of $NSNO_2$, with no energy barrier higher than that of the entrance channel. It is also possible that the reaction forms SNO + NO; this channel has a higher barrier than that found on the N_2 + SO_2 route, which is also below the entrance channel, but involves fewer isomerizations. No reaction was observed between NS and O_2 or NO, at temperatures up to 623 K and upper limits of 1×10^{-15} and 3×10^{-14} cm^3 molecule^{-1} s^{-1}, respectively, were placed on these rate coefficients.

1. Introduction

The nitrogen sulfide, NS, radical is isovalent with NO, but, unlike NO, it has been little studied and there are no direct kinetic measurements. NS was first detected in interstellar clouds using radio frequency techniques[1,2] and it has also been detected in flames using laser-induced fluorescence, LIF, by Jeffries and Crosley.[3] It is thought that the NS radical plays an important role in the interaction between nitrogen and sulfur species in flames[3] and can affect the NO_x content of exhaust gases. Wendt et al.[4] first suggested the reaction NS + O → SO + N as a primary cause of increased N_2 generation in a sulfur doped flame. Other reactions such as NS + NO → N_2 + SO and NS + N → N_2 + S,[5] have also been included in model calculations to explain the effect of sulfur on flame composition. There have been no rate coefficient measurements for any of the above reactions although estimates have been made from studies of sulfur doped flames.[4,5] The spectroscopy of NS has been characterized from several previous studies.[6−9] Particularly relevant to this study is the work by Ongstad et al.,[10] who used the photodissociation of S_4N_4 at 248 nm to produce the NS radical.

This paper reports a laser flash photolysis study of NS + NO, O_2, and NO_2, using laser flash photolysis of S_4N_4, coupled with time-resolved detection of NS using laser-induced fluorescence. The measurements are coupled with calculations of the potential energy profile.

2. Experimental Section

The slow flow, laser flash photolysis/laser-induced fluorescence system employed was similar to that used by Blitz et al.[11] and will be only briefly described. The NS radical was generated from photolysis of N_4S_4 at 248 nm using the unfocused output of an excimer laser (Lambda Physik, LPX100), with a pulse energy of ca. 200 mJ. The NS radical was probed by LIF at ∼324 nm, via the $B^2\Pi(v=1) \leftarrow X^2\Pi(v=0)$ transition using the doubled (KDP) output from a Nd:YAG (Spectron, SL803) pumped dye laser (Spectron, SL4000), operating with the dye DCM. The fluorescence was passed through a 350 nm interference filter (Ealing, bandwidth (fwhm) 10 nm) situated before the photomultiplier (EMI 9813), ensuring that the monitored fluorescence was from the resonant transition ($B^2\Pi(v=0) \rightarrow X^2\Pi(v=0)$. The signal from the photomultiplier was integrated using a boxcar averager (SRS), passed through an analogue to digital converter, and on to a personal computer for subsequent data processing. The computer delayed the time between the photolysis laser and probe laser, via a home-built pulse generator, and a kinetic trace consisted of typically 100 averaged data points. The kinetic traces were recorded between 200 μs to 20 ms, and each point determined by averaging over 4−8 samples..

Gas flows were controlled by calibrated mass flow meters (MKS) and passed into a mixing manifold before introduction into the reaction cell. The pressure in the cell was typically 5 Torr, measured via a capacitance manometer (MKS). Helium (CP grade, BOC) was used as the buffer gas. The cell was a stainless steel six-way cross with a heating block around it. The

† Part of the special issue "Donald Setser Festschrift".

* Corresponding author. Fax: ++44 113 233 6401. E-mail: m.j.pilling@chem.leeds.ac.uk.

10.1021/jp025508y CCC: $22.00
Published on Web 07/24/2002

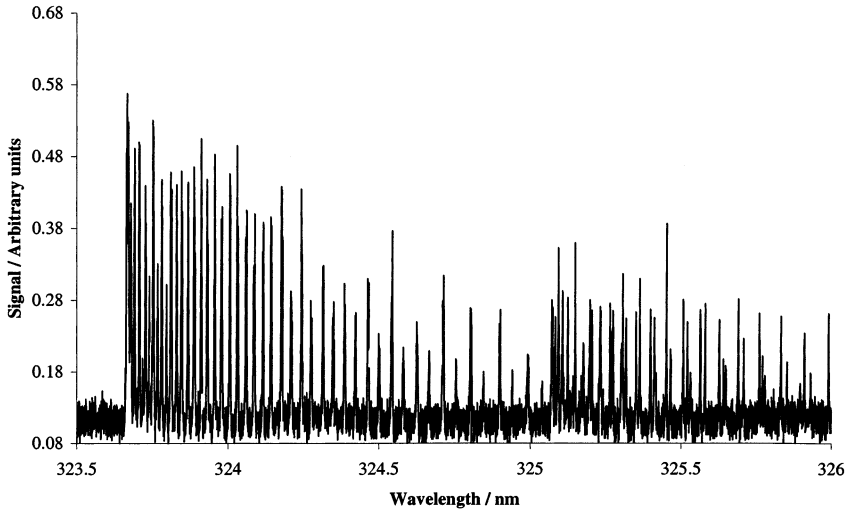

Figure 1. Excitation spectrum of the $B^2\Pi(v=1) \leftarrow X^2\Pi(v=0)$ transition of NS. The fluorescence was collected using a 350 nm interference filter.

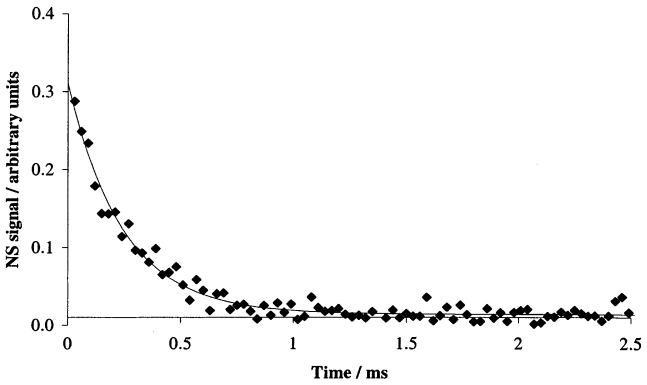

Figure 2. Decay profile for NS in the presence of 8.2 mTorr NO_2 and at total pressure of 6 Torr in a helium diluent at 373 K. The solid curve shows an exponential fit to the data.

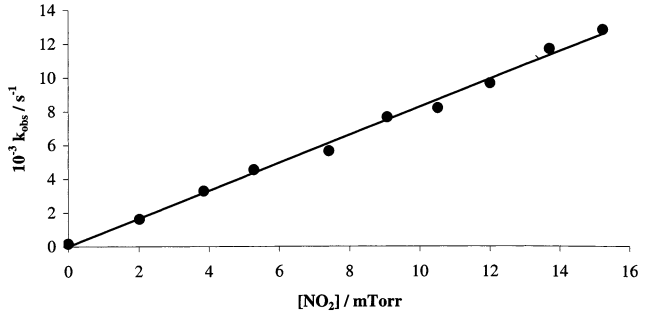

Figure 3. Plot of the pseudo-first-order decay constant for NS vs [NO_2] at 295 K and 6 Torr total pressure.

TABLE 1: Bimolecular Rate Constants for the Reaction NS + NO_2[a]

T/K	$10^{11}k_{bim}$/cm^3 $molecule^{-1}$ s^{-1}
295	2.53 ± 0.12
373	2.01 ± 0.10
473	1.84 ± 0.21
573	1.20 ± 0.06
673	1.09 ± 0.12

[a] Errors represent 2σ.

block contained cartridge heaters that allowed the cell to be heated to 700 K. The temperature was measured to ±5 K using two thermocouples located within 1 cm above and below the reaction zone, as defined by the perpendicular overlap of the two laser beams.

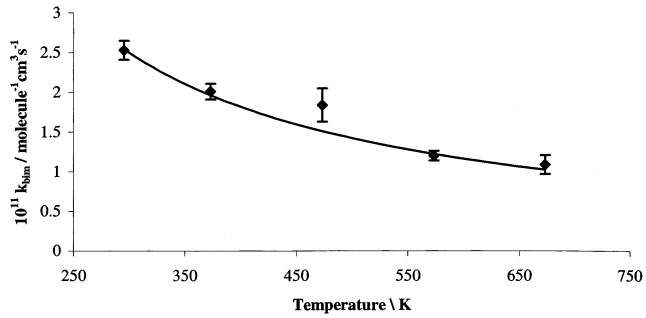

Figure 4. Temperature dependence of the rate coefficient for NS + NO_2. The error bars are the 2σ uncertainties from the plots of k_{obs} vs [NO_2]. The solid curve shows a fit to the data in the form $k = A(T/295\ K)^n$; $A = 2.57 \times 10^{-11}$ cm^3 $molecule^{-1}$ s^{-1}, $n = -1.1$

N_4S_4 was synthesized using the reaction[12]

$$[(Me_3Si)_2N]_2S + SCl_2 + SO_2Cl_2 \rightarrow {}^1/_2N_4S_4 + 4Me_3SiCl + SO_2$$

which offers a convenient route with easily removed byproducts, and no aqueous workup. In a previous study by Ongstad et al.,[10] N_4S_4 was isolated and introduced by passing the carrier gas over solid N_4S_4. This procedure requires handling the potentially hazardous crystalline form of nitrogen sulfide. In the present study, N_4S_4 was simply left dissolved in toluene, and a small amount of the N_4S_4 solution was placed in the gas inlet pipe, which connected the mixing manifold to the reaction cell. The solvent was readily pumped away, thus allowing the N_4S_4 to be entrained from the solid residue as the gas flow entered the cell. The total pressure in the cell was typically below 6 Torr in order to maintain a significant, constant concentration of N_4S_4 in the cell throughout a kinetic run. In a few experiments, where the total pressure was significantly increased, the concentration of N_4S_4 was reduced to such an extent that the kinetic traces yielded marginal information. N_4S_4 degrades at temperatures ≥473 K, giving a large-background thermal signal. This signal was removed when NO_2 was added to the cell, allowing measurements to be made up to ~673 K, when a large thermal signal returned. The decay profiles were significantly poorer at temperatures at and above 473 K than at lower temperatures.

3. Experimental Results

A fluorescence spectrum of the NS radical, $B^2\Pi(v=1) \leftarrow X^2\Pi(v=0)$, produced from the photolysis of N_4S_4 is shown in

TABLE 2: Relative Energies (kJ mol^{-1}) of Minimum Energy and Transition State (TS) Structures and Selected Bond Lengths (Å)

structure[a,b]	relative energy	bond length
(1) NS + NO_2	0[c]	N═S 1.51, N═O 1.20
(2) $NSNO_2$	−28	N═S 1.48, S—N 2.10, N═O 1.21, N═O 1.22
(3) $^{+}NS{\cdot}O_2N^{-}$	−52	N═S 1.46, S—O ∼2.3, N═O 1.25
(4) TS(2→6)	2	
(5) TS(3→6)	−32	
(6) tt-NSONO	−62	N═S 1.47, S—O 1.80, O—N 1.45, N═O 1.18
(7) TS(6→8)	−57	
(8) ct-NSONO	−64	N═S 1.47, S—O 1.77, O—N 1.49, N═O 1.17
(9) TS(8→10)	−26	
(10) cc-OSNNO	−105	O═S 1.48, S═N 1.56, N—N 1.42, N═O 1.19
(11) TS(10→12)	−60	
(12) ct-OSNNO	−88	O═S 1.47, S═N 1.58, N—N 1.40, N═O 1.21
(13) TS(12→14)	−59	
(14) cyclic-NNOS(O)	−95	O═S 1.47, S—N 1.85, N═N 1.24, N—O 1.38, O—S 1.83
(15) TS(14→16)	−82	
(16) N_2 and SO_2	−528	

[a] See Figure 5 for labeled structures. [b] Conformation is indicated by t (trans) and c (cis). [c] Zero point corrected absolute energy is −656.75128 au.

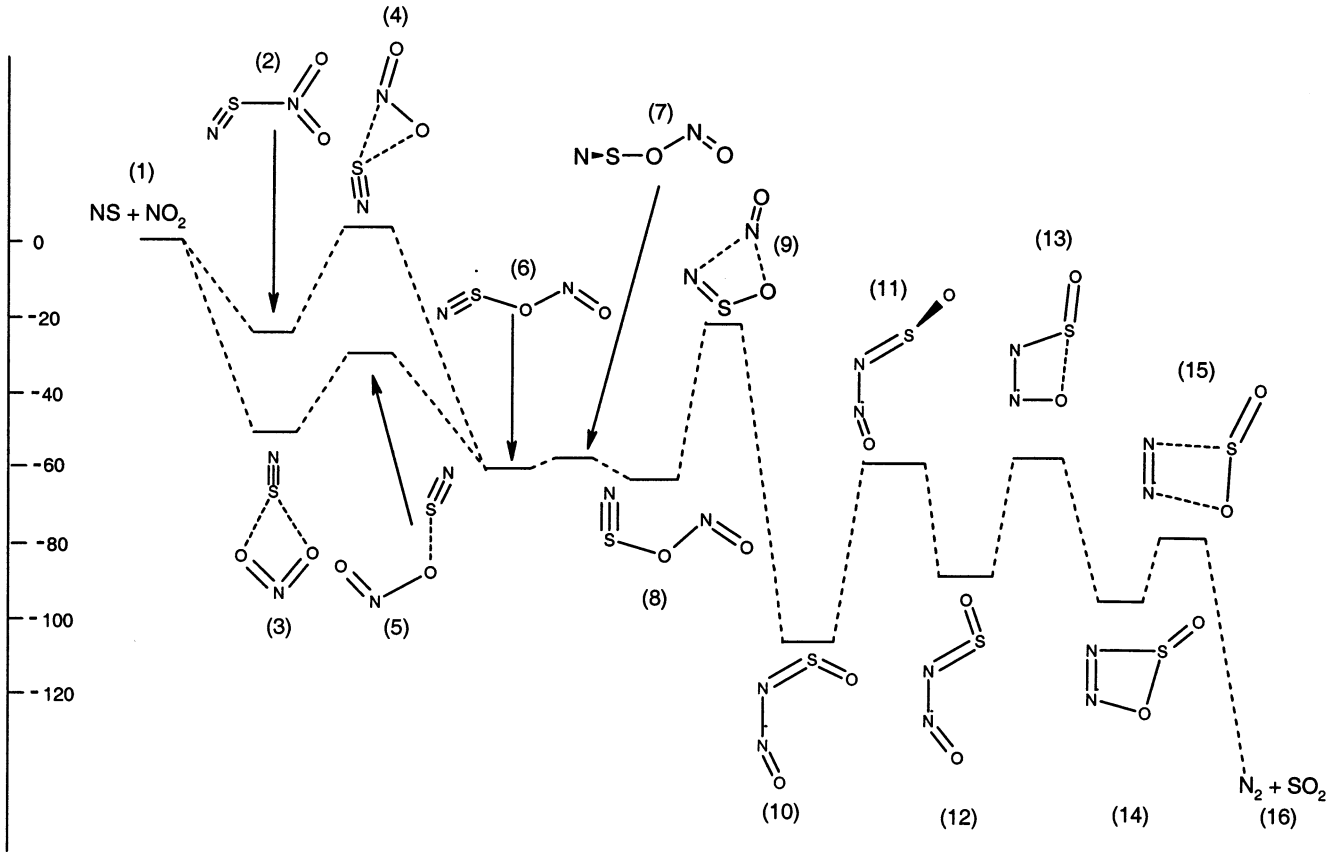

Figure 5. Calculated energies (kJ mol^{-1}) of minima and transition structures on the pathway connecting reactants (NS, NO_2) to products (SO_2, N_2).

Figure 1 This spectrum is in agreement with that recorded by Jeffries et al.[6] and by Henshaw et al.[9] who reported the production of NS on photodissociation of N_4S_4. Reactions of NS with the stable open shell species NO, O_2, and NO_2 were investigated. In the case of NO and O_2 no reaction was observed even at temperatures up to 623 K. Oxygen pressures up to 5 Torr of O_2 were examined. The decay time of NS remained at ∼1−3 ms, allowing an upper limit of 1×10^{-15} cm^3 molecules^{-1} s^{-1} to be determined for the rate coefficient. In the reaction with nitric oxide, up to 50 mTorr was added to the system, allowing an upper limit of 3×10^{-14} cm^3 molecules^{-1} s^{-1} to be assigned. The lack of reactivity between NS + O_2/NO was further evidenced by the fact that at high temperatures the thermal NS signal did not disappear on addition of either O_2 or NO.

Upon addition of NO_2 to the system a fast removal of NS was observed. Under the conditions of our experiment [NS] ≪ [NO_2] so that pseudo-first-order kinetics were observed, and an example of a kinetic trace is shown in Figure 2. The kinetic data were fitted to a single exponential and the pseudo-first-order rate constant, k_{obs}, determined. The NO_2 concentration was varied up to 20 mTorr, and the bimolecular rate constant, k_{bim}, for the reaction was obtained from a plot of k_{obs} versus [NO_2]. An example of such a plot is shown in Figure 3, where

the slope is equal to the bimolecular rate coefficient that was determined over the temperature range 293−673 K, the results being summarized in Table 1 and graphically represented in Figure 4. The 2σ uncertainties from the statistical fitting of the data, and from flow controller and other systematic errors, are given in Table 1

The temperature dependence of the rate coefficient can be expressed as

$k = (2.57 \pm 0.11) \times 10^{-11}(T/295\ \mathrm{K})^{-1.10\pm0.10}$ cm^3 molecule^{-1} s^{-1}. Limited pressure dependent experiments, in which the pressure was reduced from 6 to 2.5 Torr at room temperature, showed no dependence of the rate coefficient on pressure.

4. Potential Energy Calculations

The potential energy surface of NS and NO_2 has many minima and transition states. To locate these in an efficient manner, we have employed the density functional theory B3LYP[13,14] approach with the 6-31G** basis set.[15−19] The stationary points have been characterized by having their vibrational frequencies determined to ensure they are minima or transition states. However, although the B3LYP method usually predicts good structures, it does not always yield accurate energy differences. Thus, our strategy is to use B3LYP geometries with energies calculated by a high level ab initio method, Brueckner doubles with perturbative triples (BD(T)).[20,21] All calculations were carried out with the Gaussian suite of programs.[22]

Figure 5 displays two reaction sequences that lead to the global minimum (SO_2 and N_2), with energetics and selected bond lengths being given in Table 2. These two sequences are very similar along most of their reaction paths but differ in the nature of the initial interaction between NS and NO_2. One sequence has all intermediates, transition states, and products lower in energy than the reactants (NS and NO_2), whereas the other has one structure (4) higher in energy than the reactants but by only 2 kJ mol^{-1}. These paths consist of an initial interaction of NS and NO_2 to form (2) or (3) followed by rearrangement to a sulfur nitrite (6), which then undergoes a conformational change ((6) → (8)) followed by a 1,3 NO shift to form (10). Following another conformational change ((10) → (12)) the molecule cyclizes via transition state (13) to form (14) which then dissociates into N_2 and SO_2. We have considered these reaction sequences as they yield the global minimum products N_2 and SO_2. However, some of the single bonds in the intermediates are weak and dissociation is possible at an intermediate stage:

$$\mathrm{NS{-}O{-}NO}\ (6) \rightarrow \mathrm{NSO} + \mathrm{NO} \qquad \Delta E = +54\ \mathrm{kJ\ mol^{-1}}$$

$$\mathrm{OSN{-}NO}\ (10) \rightarrow \mathrm{OSN} + \mathrm{NO} \qquad \Delta E = +97\ \mathrm{kJ\ mol^{-1}}$$

Both reactions yield the same products, which lie below the energy of the initial reactants, NS + NO_2, by 8 kJ mol^{-1}. Most of the structures shown in Figure 5 can be rationalized by standard chemical bonding concepts. However, structure (3) has some interesting features. It can be viewed as a charge-transfer complex ($NS^{+0.38}\cdots NO_2^{-0.38}$), in which the NS bond has shortened and the NO bonds have lengthened compared to the reactants (1) (Table 2). The other initial complex (2), also has a shortened NS bond, suggesting that a triple bond exists between nitrogen and sulfur. Though it is difficult to assess the error in the calculated energies, the highest transition state in the lower energy route to N_2 + SO_2 lies 26 kJ mol^{-1} below the reactants. It is very unlikely that the errors are sufficiently large to invalidate the general conclusions discussed above.

So far we have considered reaction paths whose initial trajectories cause the sulfur atom of NS to bond to the NO_2 group. By analogy with N_2O_3, having a N−N bond and formed by the addition of NO and NO_2, the nitrogen atom of NS might be considered to be a good candidate to bond to NO_2. Although this reaction may take place, we have found that subsequent reaction paths all involve transition states whose energies lie above that of the initial reactants.

5. Discussion

Laser-induced fluorescence has been used to directly monitor the NS radical in fuel-rich methane flames by Jeffries and Crosley,[3] who observed NS only in the flame front, implying its rapid formation and destruction. Chagger et al.[5] used this observation, together with their end product sampling from a methane flame doped with NO and SO_2, to propose that the reaction NS + NO → N_2 + SO was a dominant removal channel for NS, with an estimated rate constant of 2×10^{-10} cm^3 molecule^{-1} s^{-1}. In our present study, no reaction between NS + NO was observed. A recent investigation by Hughes et al.[23] supports our conclusion; they imaged NS in a low-pressure flame doped with NH_3 and SO_2 and compared the measured vertical profiles of NS with modeled values. Much better agreement was found with low values of the rate constant for NS + NO, than with the high value proposed by Chagger et al.[5] This result differs from that of Jeffries and Crosley,[3] although the latter used an atmospheric pressure flame. No flame studies have indicated reaction between NS + O_2.

The slight negative temperature dependence of the rate coefficient for NS + NO_2 is compatible with a reaction proceeding through a bound intermediate before dissociation leads to products with no intermediate barrier higher than the entrance channel. The most energetically favorable route to products proceeds via the initial formation of the charge-transfer complex, $^{+}NS{\cdot}O_2N^{-}$ (3), which then isomerizes first to form NSONO (6) and then OSN_2O (10). Reaction to form the most stable products, N_2 + SO_2, proceeds via the cyclic isomer $O(SON_2)$ (14). The highest barrier in the reaction sequence (9) lies 26 kJ mol^{-1} below the entrance channel on the zero point surface. An alternative reaction route leads to the formation of ONS + NO by cleavage of the N−O bond in NSONO. Though this route lies only 8 kJ mol^{-1} below the reactants, it involves fewer isomerizations via tight transition states and may predominate. RRKM reactive flux calculations are being conducted on the basis of the calculated surface.

6. Conclusions

The NS radical was produced from the photolysis of N_4S_4 at 248 nm and detected via laser-induced fluorescence. No reaction was observed between NS and O_2 or NO, but a fast reaction was observed with NO_2 with $k = 2.57 \times 10^{-11}(T/295\ \mathrm{K})^{-1.1}$ cm^3 molecule^{-1} s^{-1} over the range 295−673 K. BD(T)/6-31G**//B3LYP/6-31G** calculations indicate a barrierless route to N_2 + SO_2, although formation of SNO + NO is also feasible.

Acknowledgment. We acknowledge Arto Maaninen for his help with the synthesis of N_4S_4. We thank EPSRC and DERA for funding and NERC for the award of a studentship to K. W. McKee.

References and Notes

(1) Gottlieb, C. A.; Ball, J. A.; Gottlieb, C. J.; Lada, C. J.; Penfield, H. *Astrophys. J* **1975**, *200*, L151.

(2) Kuiper, T. B. H.; Zuckerman, B.; Kakar, R. K.; Kuiper, E. N. R. *Astrophys. J* **1975**, *200*, L147.
(3) Jeffries, J. B.; Crosley, D. R. *Combust. Flame* **1986**, *64*, 55.
(4) Wendt, J. O. L.; Wootan, E. C.; Corley, T. L. *Combust. Flame* **1983**, *49*, 261.
(5) Chagger, H. K.; Goddard, P. R.; Murdoch, P.; Williams, A. *Fuel* **1991**, *70*, 1137.
(6) Jeffries, J. B.; Crosley, D. R.; Smith, G. P. *J. Phys. Chem.* **1989**, *93*, 1082.
(7) Jeffries, J. B.; Crosley, D. R. *J. Chem. Phys.* **1987**, *86*, 6839.
(8) Wysong, I. J.; Jeffries, J. B.; Crosley, D. R. *J. Chem. Phys.* **1989**, *91*, 5343.
(9) Henshaw, T. L.; Ongstad, A. P.; Lawconnell, R. I. *J. Chem. Phys.* **1992**, *96*, 53.
(10) Ongstad, A. P.; Lawconnell, R. I.; Henshaw, T. L. *J. Chem. Phys.* **1992**, *97*, 1053.
(11) Blitz, M. A.; Johnson, D. G.; Pesa, M.; Pilling, M. J.; Robertson, S. H.; Seakins, P. W. *J. Chem. Soc., Faraday Trans.* **1997**, *93*, 1473.
(12) Maaninen, A.; Siivari, J.; Suontamo, R. J.; Konu, J.; Laitinen, R. S.; Chivers, T. *Inorg. Chem.* **1997**, *36*, 2170.
(13) Lee, C.; Yang, W.; Parr, R. G. *Phys. Rev. B* **1988**, *37*, 785.
(14) Becke, A. D. *J. Chem. Phys.* **1993**, *98*, 1372.
(15) Ditchfield, R.; Hehre, W. J.; Pople, J. A. *J. Chem. Phys.* **1971**, *54*, 724.
(16) Hehre, W. J.; Ditchfield, R.; Pople, J. A. *J. Chem. Phys.* **1972**, *56*, 2257.
(17) Hariharan, P. C.; Pople, J. A. *Mol. Phys.* **1974**, *27*, 209.
(18) Gordon, M. S. *Chem. Phys. Lett.* **1980**, *76*, 163.
(19) Hariharan, P. C.; Pople, J. A. *Theor. Chem. Acta* **1973**, *28*, 213.
(20) Handy, N. C.; Pople, J. A.; Head-Gordon, M.; Raghavachari, K.; Trucks, G. W. *Chem. Phys. Lett.* **1989**, *164*, 185.
(21) Dykstra, C. E. *Chem. Phys. Lett.* **1977**, *45*, 466.
(22) Frisch, M. J.; Trucks, G. W.; Schlegel, H. B.; Scuseria, G. E.; Robb, M. A.; Cheeseman, J. R.; Zakrzewski, V. G.; Montgomery, J. A.; Stratmann, R. E.; Burant, J. C.; Dapprich, S.; Millam, J. M.; Daniels, A. D.; Kudin, K. N.; Strain, M. C.; Farkas, O.; Tomasi, J.; Barone, V.; Cossi, M.; Cammi, R.; Mennucci, B.; Pomelli, C.; Adamo, C.; Clifford, S.; Ochterski, J.; Petersson, G. A.; Ayala, P. Y.; Ciu, Q.; Morokuma, K.; Malick, D. K.; Rabuck, A. D.; Raghavachari, K.; Foresman, J. B.; Cioslowski, J.; Ortiz, J. V.; Stefanov, B. B.; Liu, G.; Liashenko, A.; Piskorz, P.; Komaromi, I.; Gomperts, R.; Martin, R. L.; Fox, D. J.; Keith, T.; Al-Laham, M. A.; Peng, C. Y.; Nanayakkara, A.; Gonzalez, C.; Challacombe, M.; Gill, P. M. W.; Johnson, B. G.; Chen, W.; Wong, M. W.; Andres, J. L.; Head-Gordon, M.; Replogle, E. S.; Pople, J. A. *Gaussian98*, revision E.7; Gaussion Inc.: Pittsburgh, PA, 1998.
(23) Hughes, K. J.; Tomlin, A. S.; V. A. Dupont and M. Pourkashanian *Faraday Discuss.* **2001**, *119*, 337−352